

Coconut shell-derived activated carbon for NIR photo-activated synergistic photothermal-chemodynamic cancer therapy

Gang Wu, †,^a Bao Jiang, †,^a Lin Zhou, ^a Ao Wang, *,^b and Shaohua Wei *,^{a,c}

^a *College of Chemistry and Materials Science, Jiangsu Key Laboratory of Bio-functional Materials, Jiangsu Collaborative Innovation Centre of Biomedical Functional Materials, Key Laboratory of Applied Photochemistry, Nanjing Normal University, Nanjing 210023, China.*

^b *Institute of Chemical Industry of Forest Products, Chinese Academy of Forestry, Nanjing 210042, China.*

^c *School of Chemistry and Chemical Engineering, Yancheng Institute of Technology, Yancheng 224051, China.*

* *Corresponding author. Email: wangao@icifp.cn (A. Wang); shwei@njnu.edu.cn (S. H. Wei)*

† *G. Wu and B. Jiang contributed equally to this work.*

1. Experimental Details

1.1. Chemicals and instruments

3,3',5,5'-Tetramethylbenzidine (TMB), 5,5-dimethyl-1-pyrroline N-oxide (DMPO), 2-hydroxyterephthalic acid, terephthalic acid and vitamin C were purchased from Aladdin (China). Acetate (HAc), 30% hydrogen peroxide (H₂O₂), sodium acetate

(NaAc), polyvinylpyrrolidone (PVP, k30) and anhydrous dimethyl sulfoxide (DMSO) were all purchased from Sinopharm Chemical Reagent Co., Ltd. (China). 3-(4,5-dimethyl-2-thiazolyl)-2,5-diphenyl-2-H-tetrazolium bromide (MTT), the Annexin V, FITC Apoptosis Detection Kit, and 2,7-Dichlorodihydrofluorescein diacetate (DCFH-DA) were purchased from Beyotime (China). The lysosome probe Lyso-Tracker blue was purchased from Thermo Fisher. Dulbecco's modified eagle medium (DMEM) was from Gibco (USA). Newborn calf serum (NBS) was from Tianhang (China). Hematoxylin and eosin (H&E) stain Kit were from Shanghai Yisheng (China). Besides, deionized water was used throughout the experiment. All reagents were analytical grade and obtained from commercial suppliers, which used directly without further purification.

The UV spectrum of the sample was detected with A Cary 50 spectrophotometer (Varian, USA). Transmission Electron Microscope (TEM) images were recorded with JEM-2100 microscopy (Hitachi, Japan, 80 kV accelerating voltage). X-ray photoelectron spectroscopy (XPS, ESCALab 250Xi, Thermo Fisher Scientific, USA) analyzed the composition and content of elements. The complex examination's metal loading was performed using an Inductively coupled plasma atomic emission spectrometer (ICP, Prodigy, USA). Specific surface area and pore volume are tested on the surface area analyzer (ASAP2460, Mike Instruments Inc, USA). The detection of oxidized hydroxyl radicals ($\cdot\text{OH}$) was obtained by Electron spin resonance spectroscopy (Japan Electronics, JES-FA300). The size distribution of nanomaterials was recorded using a Zetasizer Nano ZS90 (Malvern Instruments) through dynamic

light scattering (DLS). A high-temperature tube furnace (GSL-1500X-OTF, Hefei Kejing Material Technology Co., Ltd, China) was used in carbon materials' carbonization and activation. Ultrafine particle crusher (MKCA6-5J, MASUKO SANGYO CO., LTD. Japan) and High-pressure microfluidization homogenizer (Nano LAB TYPE, Noozle Fluid Technology Co., Ltd, China) had done further ball milling work on carbon materials. Fluorescence microscope images were acquired with confocal laser scanning microscopy (CLSM, Nikon Eclipse Ti). Cell counting was recorded by a microplate reader (Thermo, USA). Flow cytometry (FCM) tests were obtained with XL flow cytometer (Beckman, USA). Magnetic resonance imaging (MRI) experiments were performed on a low-field animal MRI system (NIUMAG MesoMR23-060H-I). The photothermal performance data were obtained with 808 nm laser (0.30, 0.50, 0.75, or 1.00 W cm⁻²) and FLIR-E5 (Sweden).

1.2. Cell culture and animals

4T1, a mouse breast cancer cell line, and NRK (rat kidney cell line) were purchased from the Cell Bank of the Chinese Academy of Sciences (Shanghai, China). 4T1 cancer cells and NRK, containing DMEM with 10% inactivated NBS were cultured in a constant temperature incubator (37 °C, 5% CO₂, 95% air). Balb/c mice (5-6 weeks, ~20 g, female) were purchased from Hangzhou Zi yuan Experimental Animal Technology Co., Ltd (China). All purchased animals were approved by the Nanjing Normal University Animal Ethics Committee Guidelines (China). Additionally, the animal's entire experiments were followed institutional guidelines of the Animal Ethics

Committee of Nanjing Normal University (China) and performed in compliance with the regulations for the Administration of Affairs Concerning Experimental Animals of China.

1.3. Photothermal conversion efficiency

We calculated the photothermal conversion efficiency (η) of PANs according to the literature method. The calculation formula was as follows according to previous work ¹:

$$\eta = \frac{h s (T_{Max} - T_{Surr}) - Q_s}{I (1 - I_0 - A_{808})} \times 100\%$$

Firstly, PANs (100 $\mu\text{g mL}^{-1}$) were measured after being configured in an aqueous solution irradiated by 808 nm laser (1.00 W cm^{-2}) until it reached a steady state. The temperature change of the sample solution made use of an infrared thermal imager to record. Its η value was derived from the above formula.

Where h and s are the heat transfer coefficient and the container surface area, respectively. The maximum stable temperature (T_{Max}) and the environmental temperature (T_{Surr}) were 64.20 $^{\circ}\text{C}$, 23.00 $^{\circ}\text{C}$, respectively. The Q_s has represented the heat emitted by the light absorbed from the container itself. Its value was 16.20 mW. The laser power (I) was 1.00 W cm^{-2} , and the PANs of absorbance at 808 nm (A_{808}) was 0.90.

The parameter θ was calculated by the following formula:

$$\theta = \frac{T - T_{Surr}}{T_{Max} - T_{Surr}}$$

According to the cooling curve of the sample and the following formula, the time constant τ_s was 419.31 s.

$$t = -\tau_s \ln \theta$$

$$hs = \frac{m_D C_D}{\tau_s}$$

Where m_D (1ml water) is 1 g, C_D (specific heat capacity of water) is $4.20 \text{ J g}^{-1}\text{ }^\circ\text{C}^{-1}$. Consequently, according to the above formula, hs is $412 \text{ mW } ^\circ\text{C}^{-1}$. Therefore, the η value of PANs was 45.20%.

1.4. Electron spin resonance (ESR) spectroscopy measurement

The detection of $\cdot\text{OH}$ was carried out with electron spin resonance spectroscopy. All experiments were divided into four groups: (1) Control, (2) Gd@PANs, (3) Gd@PANs + 808 nm laser (1.00 W cm^{-2}), (4) Gd@PANs+323K ($[\text{PANs}] = 50 \mu\text{g mL}^{-1}$, $[\text{gadodiamide}] = 9.80 \mu\text{g mL}^{-1}$). They were all implemented under the conditions of pH 4.5 and H_2O_2 (1mM) with DMPO as a capture agent. 200 microliter sample solution was placed in a glass capillary with an inner diameter of 1mm and sealed (12 min). Before the experiment, the capillary was inserted into the ESR cavity and the spectra was recorded. The relevant parameters are as follows: frequency: 9.853 Ghz, power: 19.8 mw, center field: 3400 G, sweep width: 2000 G, mod amplitude: 1G, time constant: 1.250 ms, sweep time: 69.456 s.

1.5. The stable performance test of Gd@PANs

The Gd@PANs was dispersed in water or PBS buffer for 1, 2, and 3 days, respectively. Then, the Gd@PANs were collected by centrifugation and redispersed in the water again. After that, the T1-MRI signal strength and zeta potential of Gd@PANs were detected.

1.6. Hydroxyl radicals ($\cdot\text{OH}$) quantitative detection

Terephthalic acid (TA) can react with $\cdot\text{OH}$ to generate 2-hydroxyterephthalic acid, which can be excited by 315 nm light to produce a 435 nm fluorescence signal ². According to the standard curve of the generated fluorescent substance (2-hydroxyterephthalic acid), the $\cdot\text{OH}$ concentration generated by the reaction of Gd@PANs and H_2O_2 can be obtained ³.

1.7. Cell uptake rate and subcellular location detection

Gd@PANs was diluted to $30 \mu\text{g mL}^{-1}$ by colorless DMEM, and the detected absorbance at 808 nm is recorded as A1. 4T1 cells were seeded in a 24-well plate, after incubating at 37°C for 24 h, the original culture medium was removed. Next, Gd@PANs ($30 \mu\text{g mL}^{-1}$) was diluted with colorless DMEM and added to a 24-well plate, placed at 4°C and 37°C , respectively. After 24 h, the supernatant was collected and placed in a micro cuvette to test the absorbance of the sample, and it was recorded as A2. The uptake rate (W) of the cell to the drug was calculated via the equation:

$$W = \frac{A1 - A2}{A1} \times 100\%$$

In addition, nystatin (NYS), amiloride (AMI), and chlorpromazine (CPZ) are used as three kinds of endocytosis inhibitors, respectively. They were added to the cells and

incubated for 1 h before Gd@PANs incubation, and then the cell uptake rate is calculated according to the above formula.

The 4T1 cells were incubated into the glass bottom petri dish for 24 h. The medium was then removed, the PANs ($15 \mu\text{g mL}^{-1}$) and Gd@PANs ($[\text{PANs}] = 15 \mu\text{g mL}^{-1}$, $[\text{gadodiamide}] = 2.94 \mu\text{g mL}^{-1}$) diluted with a new medium was added. After 24 h of incubation, Lyso-Tracker blue (EX = 470 nm, 100×10^{-9} M) and Mito-tracker green (EX = 488 nm, 100×10^{-9} M) was diluted with DMEM and added to cells for 0.5 h. Before the experiment, the cell culture dish was washed three times by PBS, and then it was imaged with confocal laser scanning microscopy.

2. Results and discussion

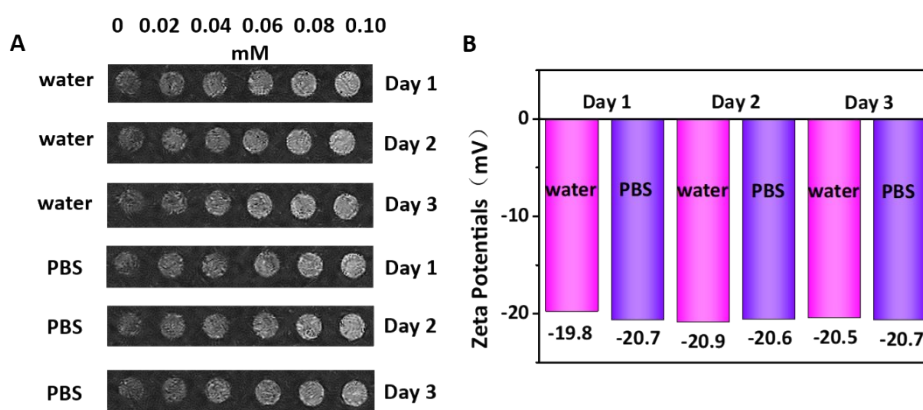


Fig. S1. T1-MRI signal (A) and zeta potential (B) changes of the Gd@PANs in water or PBS buffer for 1, 2, and 3 days, respectively.

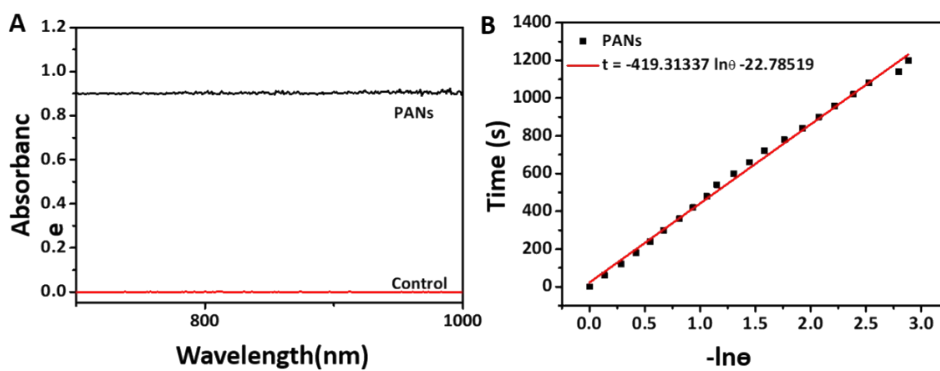


Fig. S2. The absorption spectra (A) and cooling curve fitting (B) of PANs.

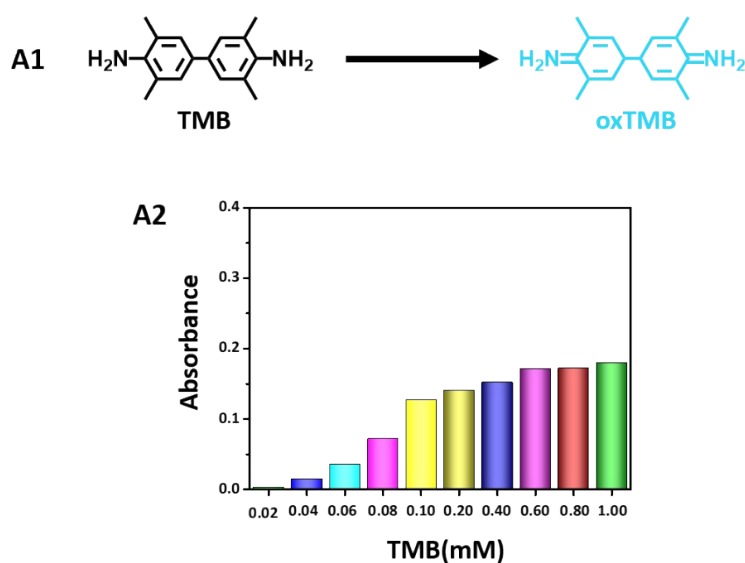


Fig. S3. (A1) The simple intention of TMB being oxidized to oxTMB. (A2) The absorbance intensity of oxidized TMB in the presence of H_2O_2 (0.5 mM) and Gd@PANs ($50 \mu\text{g mL}^{-1}$) with various TMB concentrations.

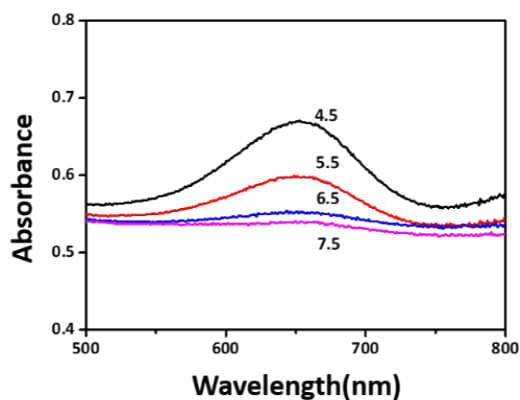


Fig. S4. The absorbance curve of TMB (0.6 mM) in the presence of H₂O₂ (0.5 mM) using Gd@PANs at different pH values.

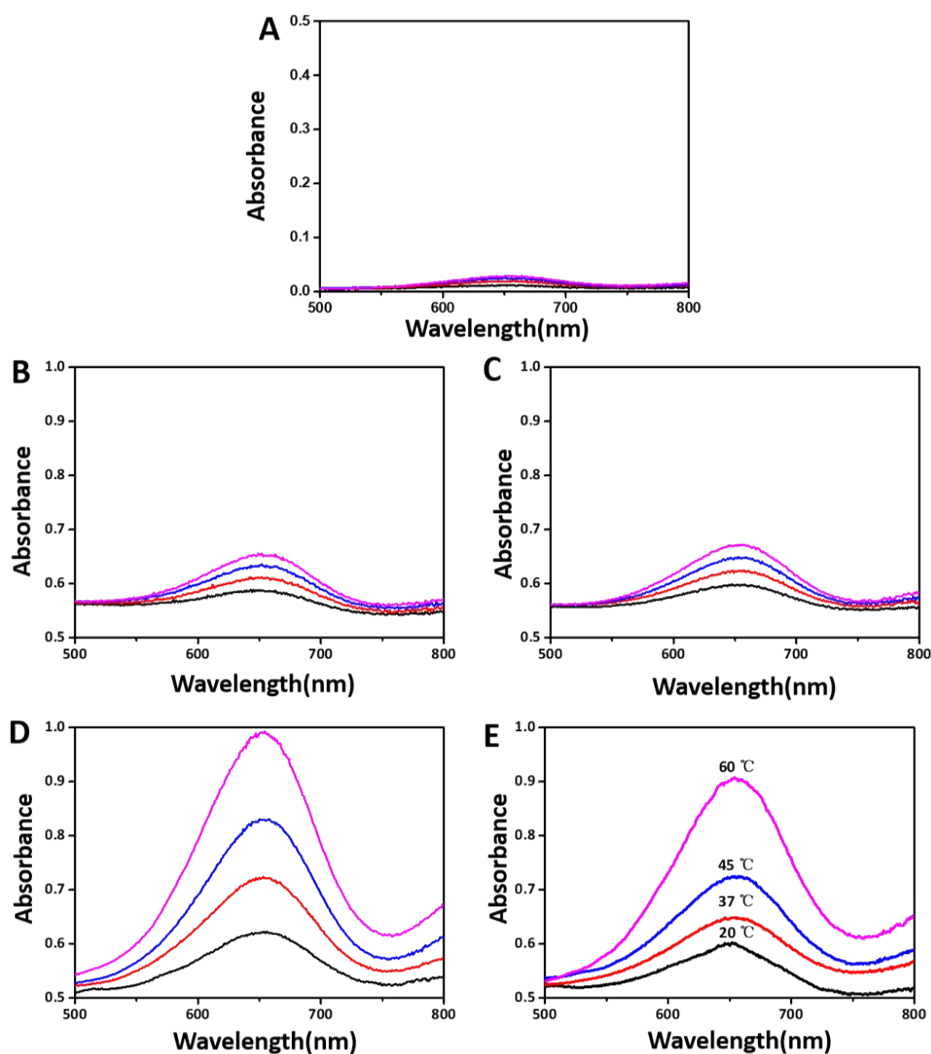


Fig. S5. The absorbance curve (3-12 min) of TMB (0.6 mM) in the presence of H₂O₂ (0.5 mM) with gadodiamide (A), PANs (B), Gd@PANs (C), Gd@PANs under 808 nm laser (D), different temperature (E).

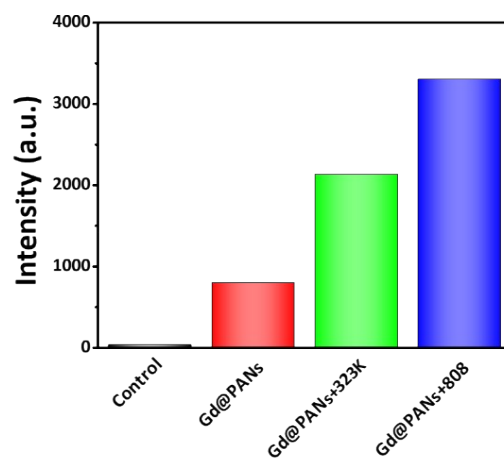


Fig. S6. The comparison of the ESR signal of Gd@PANs under different conditions with magnetic field of 3239.2149 (G).

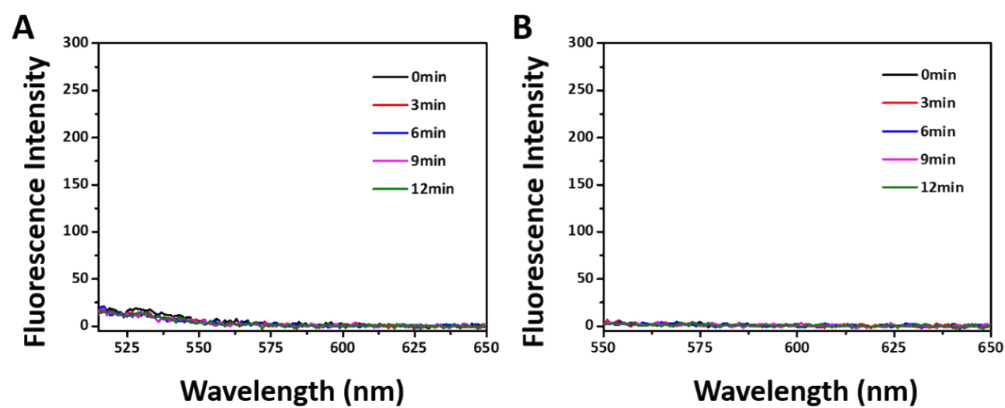


Fig. S7. Fluorescence spectra changing of SOSG (A) and DHE (B) incubated with Gd@PANs ($50 \mu\text{g mL}^{-1}$) in the presence of H_2O_2 (0.5 mM).

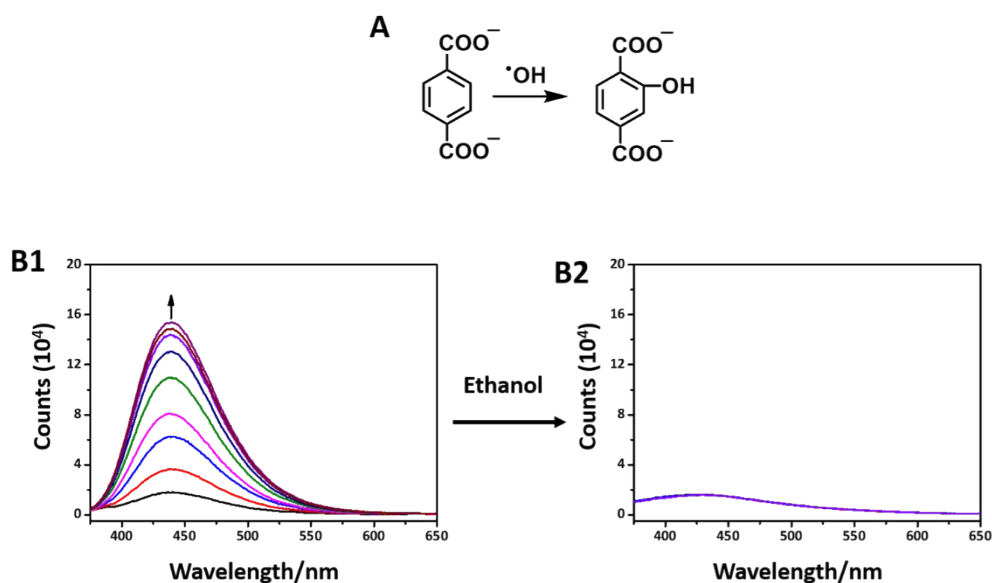


Fig. S8. (A) Schematic representation of detection of $\cdot\text{OH}$ by TA. The incubation time-dependent fluorescence spectra change of the mixture of TA (0.4 mM), Gd@PANs ($50 \mu\text{g mL}^{-1}$), and H_2O_2 (0.5 mM) in the absence (B1) or presence (B2) of ethanol.

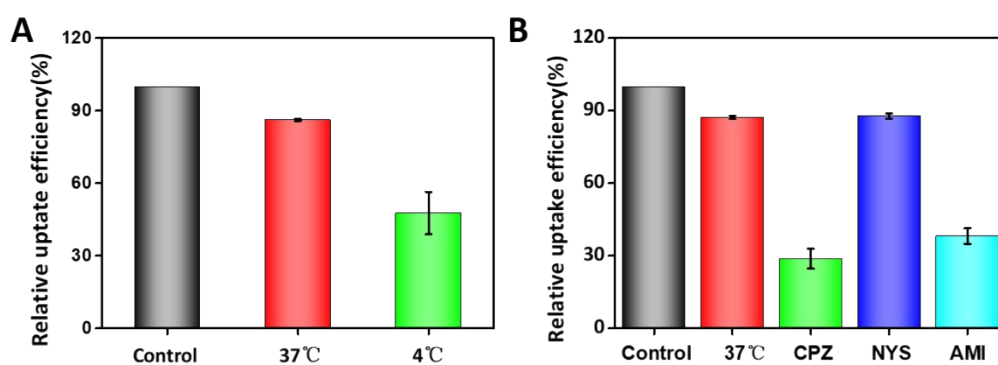


Fig. S9. (A) The cellular uptake efficiency comparison of Gd@PANs at 4 °C and 37 °C; (B) The cellular uptake efficiency comparison of Gd@PANs at 37 °C and in the presence of CPZ, NYS, AMI as endocytosis inhibitor ($[\text{Gd@PANs}] = 30 \mu\text{g mL}^{-1}$, $[\text{CPZ}] = 2 \mu\text{M}$, $[\text{NYS}] = 2.5 \mu\text{g mL}^{-1}$, $[\text{AMI}] = 100 \mu\text{M}$).

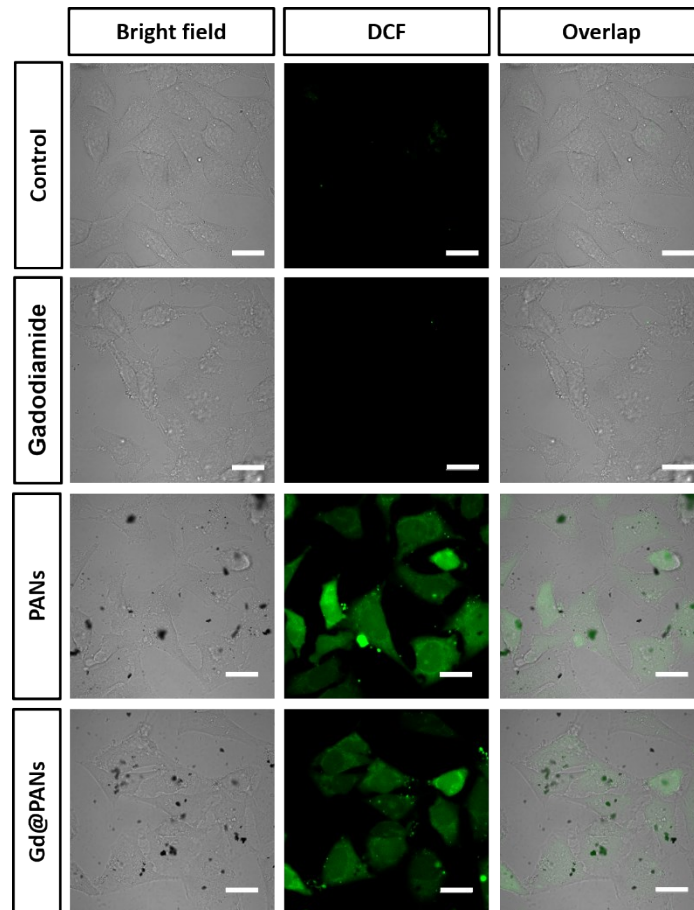


Fig. S10. CLSM images of DCFH-DA stained 4T1 cells post treating by Gadodiamide, PANs and Gd@PANs (scale bar = 20 μm).

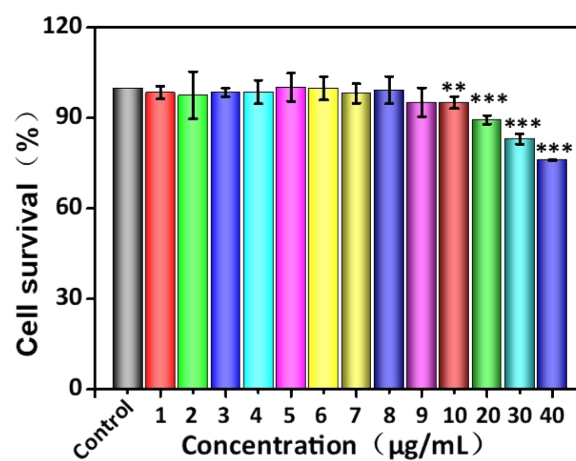


Fig. S11. The relative cell survival rate of 4T1 cells post treating by different concentrations of Gd@PANs (**P < 0.01, ***P < 0.001, Gd@PANs treated group

versus control).

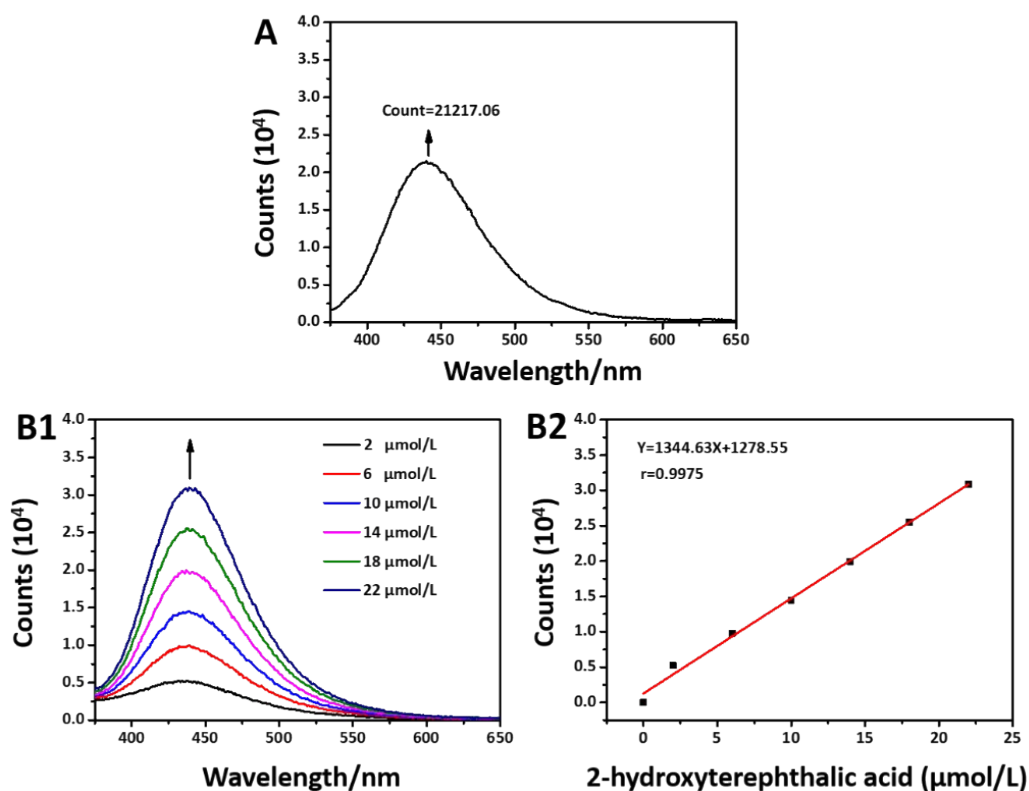


Fig. S12. (A) The complete reaction between Gd@PANs ($10 \mu\text{g mL}^{-1}$) and H_2O_2 (0.1 mM) induced the fluorescence signal of 2-hydroxyterephthalic acid. Fluorescence spectra of 2-hydroxyterephthalic acid at the various concentration (B1) and their linear fitting curve (B2).

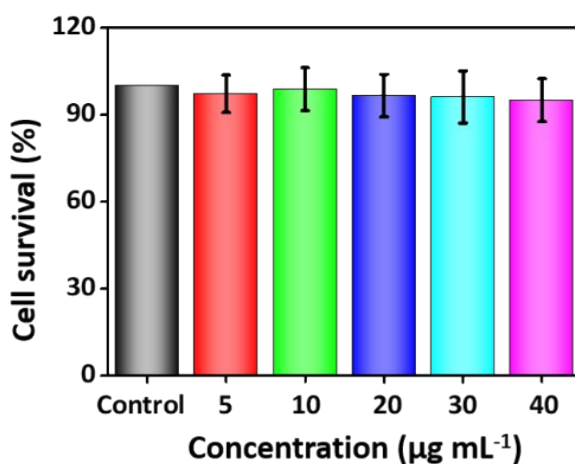


Fig. S13. 4T1 cell survival rate post co-treating by different concentrations of PANs

with vitamin C.

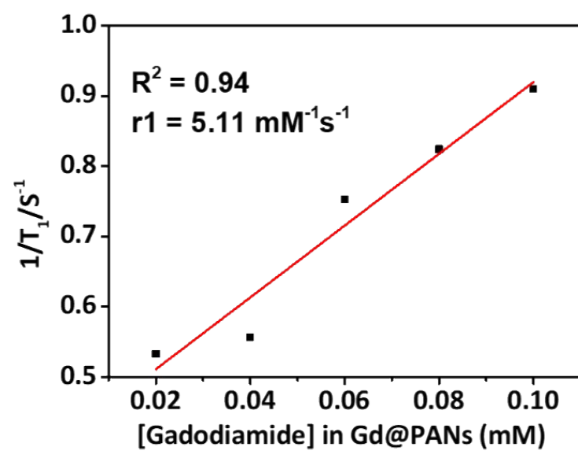


Fig. S14. The relaxation rate parameter ($r1$) of gadodiamide under various concentrations.

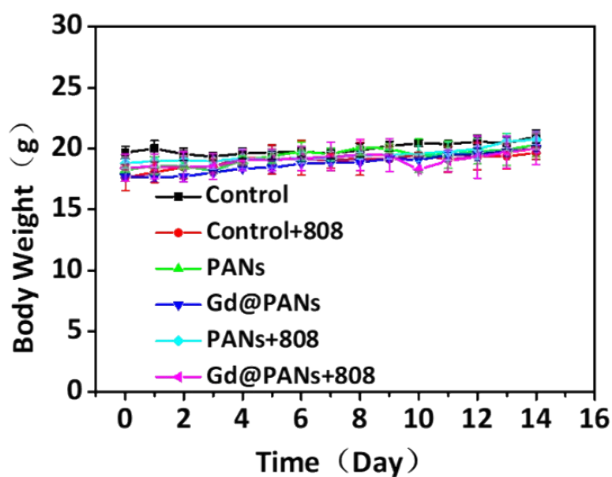


Fig. S15. The changes in body weight of mice treated with various drugs in each group during 14 days.

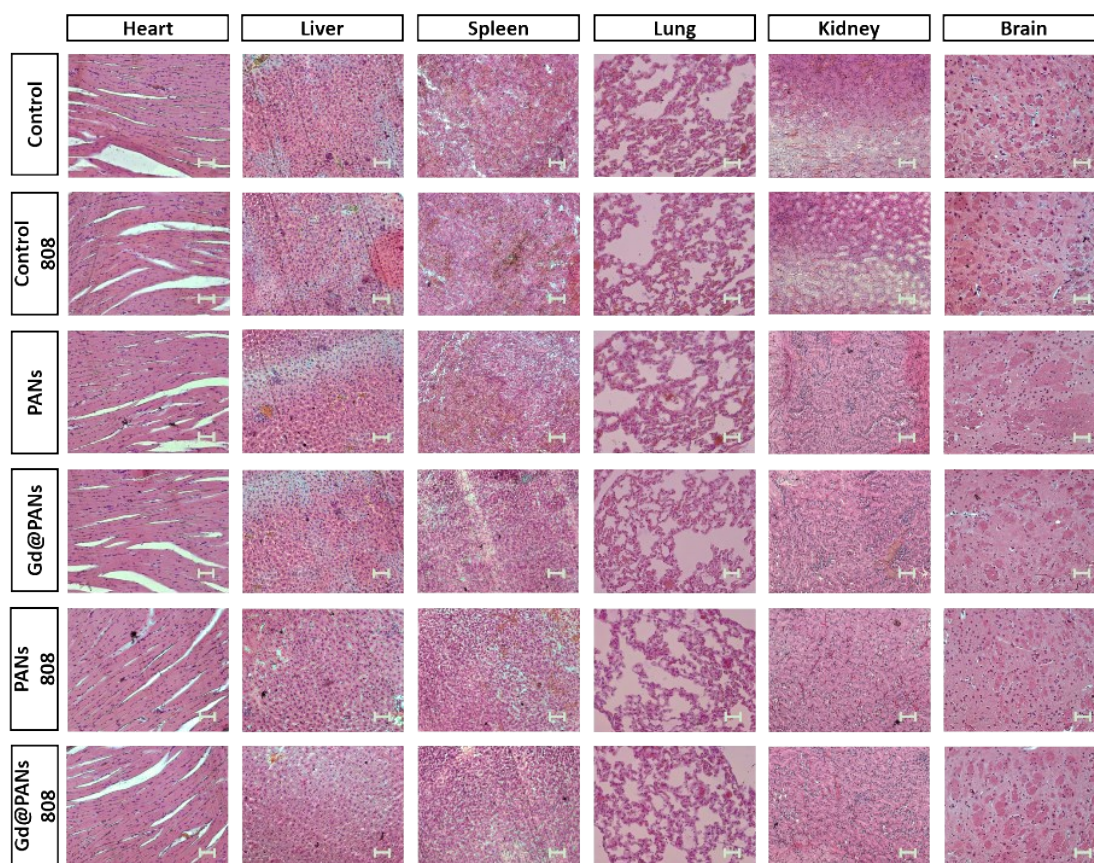


Fig. S16. H&E staining of microscopy images of the main organs (heart, liver, spleen, Lung, kidney, and brain) after various treatments (scale bar = 50 μm).

Table S1. Surface area and total volume in pores from BET analysis.

| Sample | BET Surface Area ($\text{m}^2 \text{g}^{-1}$) | Total Volume in Pores ($\text{cm}^3 \text{g}^{-1}$) |
|---------|---|---|
| ANs | 2478.09 | 1.19 |
| Gd@ANs | 1021.48 | 0.50 |
| Gd@PANs | 819.93 | 0.40 |

Table S2. Synergistic index of PTT-CDT treatment with PANs or Gd@PANs.

^a Mean growth inhibition rate (MGI) = survival cell percent of treated group / survival cell percent of control group. Expected $MGI_{PTT-CDT} = (MGI_{CDT} \times MGI_{PTT}) / 100$. Synergistic index = Expected $MGI_{PTT-CDT} /$ Observed $MGI_{PTT-CDT}$. Synergistic index > 1 indicates there is synergistic effect in the combination treatment. Synergistic index <

| Samples | Additive and synergistic effect | | | | |
|---------|---------------------------------|------------------------|----------------------------|----------|-------------------|
| | MGI _{CDT} (%) | MGI _{PTT} (%) | MGI _{PTT-CDT} (%) | | Synergistic Index |
| | | | expected | observed | |
| PANs | 81.02 | 58.97 | 47.77 | 35.99 | 1.33 |
| Gd@PANs | 79.45 | 59.54 | 47.30 | 33.17 | 1.43 |

1 indicates there is no synergistic effect in the combination treatment.⁴

References

- 1 Y. Cheng, X. Tan, J. Wang, Y. Wang, Y. Song, Q. You, Q. Sun, L. Liu, S. Wang, F. Tan, J. Li and N. Li, *J. Control. Release.*, 2018, **277**, 77-88.
- 2 E.G. Ju, K. Dong, Z.W. Chen, Z. L, C.Q. Liu, Y.Y. Huang, Z.Z. Wang, F. Pu, J.S. Ren and X. G. Qu, *Mol. Angew. Chem.* 2016, **128**, 11639-11643.
- 3 S.Y. Wang, X. Ding, X.H. Zhang, H. Pang, X. Hai, G.G Zhan, W. Zhou, H. Song, L.Z. Zhang, H. Chen and J.H. Ye, *Adv. Funct. Mater.* 2017, 1703923.
- 4 D.H. Shin, H.-Y. Min, A.K. El-Naggar, S.M. Lippman, B. Glisson and H.-Y. Lee, *Mol. Cancer. Ther.*, 2011, **10**, 2437-2448.